ANALYSIS OF THE SPECTRA AND REDOX PROPERTIES OF PURE CYTOCHROMES aa_3

RICHARD W. HENDLER,* K. V. SUBBA REDDY,* RICHARD I. SHRAGER,‡ AND W. S. CAUGHEY§
Laboratory of Cell Biology, National Heart, Lung, and Blood Institute and ‡Laboratory of Applied Studies, Division of Computer Research and Technology, National Institutes of Health, Bethesda, Maryland 20892; and §Department of Biochemistry, Colorado State University, Fort Collins, Colorado 80523

ABSTRACT The findings in the current studies with pure cytochrome aa_3 confirm the findings in an accompanying paper pertaining to cytochrome aa_3 in mitochondria (Reddy et al., 1985). In both cases, three Nernstian titrations are seen with E_m values near 200, 260, 340 mV with n values of 2, 2, and 1. Similarly, the α absorption features of the difference spectra in both cases were centered near 602, 605, and 607 nm. The component with E_m ~200 mV was identified as heme a_3 on the basis of experiments conducted in an atmosphere of carbon monoxide, and in both cases, the carbon monoxide-liganded species did not display an elevated E_m. In the current studies, unique Soret absorbance features are added to the difference spectra for the three Nernstian transitions. Specifically, absorption peaks at 429, 446, and 448 nm go with the α peaks seen respectively at 602, 605, and 607 nm. Evidence was presented to support the hypothesis that the redox state of heme a may control the redox potential of heme a_3.

INTRODUCTION

This paper is the fifth in a series of studies designed to reexamine the spectral and thermodynamic properties of mammalian cytochromes, using more rigorous techniques of data collection and analysis (Reddy and Hendler, 1983; Shrager and Hendler, 1982; Reddy and Hendler, 1986; Reddy et al., 1986). It is the complement of a study of cytochrome oxidase in situ in mitochondria (Reddy et al., 1986). The results regarding the α absorption feature of the enzyme, have been found to be the same with the pure enzyme as were found with the enzyme in situ. The current study extends the characterization to include the behavior of the Soret absorption region. Cytochrome a_3 has been identified as a 190 mV component with n value of 2, a Soret peak at 429 nm and an α absorbance of 602 nm in reduced oxidized difference spectra. Evidence is presented that the E_m of this cytochrome may be controlled by the redox state of heme a. In addition to the 190 mV species, it is found that in confirmation of the in situ studies (Reddy et al., 1986), an $n = 2$ component with an E_m of 260 mV and an $n = 1$ component with an E_m of 340 mV are present. The current findings are considered in relation to previous ideas on the thermodynamic properties of the enzyme and schemes to accommodate the newer findings are presented. Effects of changes in pH and of various ligands were studied.

EXPERIMENTAL PROCEDURES

The source of mediators and other chemicals, as well as the titration procedures and apparatus, spectrometer and general procedures are as previously described (Reddy and Hendler, 1986; Reddy and Hendler, 1983). In order to be able to study both the α band region near 604 nm, and the Soret band region near 440 nm, an important modification of the spectrometer set-up was required. The tungsten iodide light source provides only a small fraction of illumination in the Soret region compared to the α region. Even with the exposure in the α region at near the saturation level of the photodiode detectors, insufficient illumination was available in the Soret region. This situation was rectified by using color conversion filters (a Kodak Wratten 80A gelatin conversion filter plus a Hoya HMC multi-coated glass 80A filter) which passed more of the wavelengths in the Soret region than the wavelengths of the α region. By increasing the illumination of the source, a converted spectrum was then available which gave sufficient illumination of the whole wavelength spectrum including both regions of interest. The methods of data analysis are as previously described (Shrager and Hendler, 1982; Reddy and Hendler, 1983; Shrager and Hendler, 1986). These include the use of the second derivative of absorbance centered on specific absorption regions and the SVD method of analysis. Cytochrome aa_3 was isolated from bovine heart muscle by the method of Yoshikawa et al. (1977) and stored at a concentration of 1.6 mM at −80°C in 10 μl aliquots. A homogenate of fresh chicken egg was made by directly homogenizing the raw egg at low speed in a motor driven homogenizer. This preparation which usually contained about 80 mg of protein per ml was stored in aliquots at −80°C. This preparation was present at a concentration of 5 mg protein per ml where noted, in order to protect the pure enzyme from various types of surface denaturation including possible deleterious interactions with the working electrode. An additional role for the egg homogenate was to provide a mixture of lipoproteins and lipids for the enzyme, which normally functions in a membrane environment. Beef liver catalase was obtained from Boehringer Mannheim Biochemicals (West Germany) and equine heart cytochrome c from Sigma Chemical Co. (St. Louis, MO). For carbon monoxide experiments, the system was first made anaerobic with argon in the usual manner. After making adjustments to the reaction cuvette and stirring apparatus, the gas was switched to carbon monoxide. The reaction cuvette was enclosed in a custom made hood. The gas was played over the surface of the stirred solution for 30 min prior to the start of the titration and continuously throughout the whole experiment. A description of all of the experiments and the composition of the incubation medium are given in Table I. In addition to the usual titration procedures

Please address all correspondence to Richard W. Hendler.

TABLE I
DESCRIPTION OF THE EXPERIMENTS

Exp. No.	Type	Method*	Voltage range	Number of spectra analyzed	Exp. No.	Type	Method*	Voltage range	Number of spectra analyzed
			mV		117	cyanide	CR	464–93	94
118	control	CR	450–95	90	136	cyanide	ER	455–112	108
119	control	CR	462–98	106	155	cyanide	EO^P	104–454	55
124	control	CR	468–103	92	156¶	cyanide	ER	424–100	76
128	control	CR	449–48	101	158¶	cyanide	ER	461–109	80
132§	control	ER	454–92	85		azide			
133‖	control	ER	481–104	78	94	azide	CR	457–99	73
145	control	EO	96–452	58	95	azide	EO**/CO	117–444	73
146	control	EO^P	100–465	68	96	azide	CR	459–105	77
148‡	control	ER^P	294–93	30	97	azide	CO	126–449	70
		EO^P	104–452	61	137	azide	CR	444–97	84
149‡	control	ER^P	396–100	53	161	azide	ER^P	448–153	51
		EO^P	105–475	24	162	azide	EO^P	100–426	64
150‡	control	ER^P	290–93	34	163	azide	ER^P	436–105	54
		EO^P	101–453	43					
151‡	control	EO^P	93–444	65	129	Carbon monoxide	CR	447–48	101
152	control	ER^P	291–103	30					
		EO^P	93–263	26	130	Carbon monoxide	CR	450–33	109
153	control	ER	445–94	40					
154‡	control	ER^P	455–118	53		Mediator control			
157	control	CR	465–126	78					
139	pH 8.0	CR	440–51	97	108	(+egg)	ER	477–110	97
140	pH 8.0	CR	460–37	106	121	(+egg)	EO	129–435	60
142	pH 8.0	CR	461–54	94	122	(−egg)	EO	78–449	115
141	pH 6.0	CR	429–102	88	127	(−egg)	CR	466–95	80
143	pH 6.0	CR	442–101	87					

Control experiments contained 5.3 μM cytochrome oxidase in 3 ml of a medium containing 125 mM KCl, 62.5 mM potassium phosphate and mediators at pH 7.0. Unless otherwise noted 15 mg of protein of a total homogenate of chicken egg was also present in order to protect the enzyme from denaturation. The mediators present were potassium ferricyanide and quinhydrone at 0.2 mM each, and diaminodurene, 1,2-naphthoquinone and phenazine methosulphate at 0.1 mM each. The mediator controls contained the buffer and mediator plus 17.2 mg of protein of the egg homogenate. For the experiments at pH 6.0, MES (66.5 mM) was present and the pH was adjusted with 1N HCl. For the experiments at pH 8.0, Tris (66.5 mM) was present and the pH was adjusted with 1M NaOH. Cyanide was present at 1 mM and azide at 10 mM. Carbon monoxide experiments were conducted under an atmosphere of the pure gas used in place of argon. Equilibration of the medium with the gas phase was achieved by pregassing the stirred medium for at least 30 min.

*The methods of titration were CR (chemical reduction), ER (electrical reduction using a constant current generator), ER^P (electrical reduction using a potentiostat), EO (electrical oxidation using a protentiostat). In experiments 148 to 152 inclusive, both a reductive and an oxidative titration were performed on the same sample in succession. Each titration phase is shown separately in the table. These methods are more fully described in Methods and in references.

‡Egg homogenate was not present.

§Catalase (50 nM, 697 units/ml) was present.

‖1 mM H_2O_2 was present.

¶Incubated with cyanide overnight.

**The electrical oxidation employed the constant current generator.

which included chemical reduction and electrical oxidation and reduction, a new technique was employed. Because of the possibility that the pure soluble enzyme might suffer undesirable effects by direct interaction with high or low voltages on the working platinum electrode, a different principal was employed in most of the electrical titrations. The electrical titration system already described uses a constant current generator to drive the working platinum electrode. In the new system, a potentiostat is used to set and maintain desired voltages on the platinum electrode.

The potentiostat utilized a National Semiconductor LH0042 operational amplifier to drive the auxiliary Ag/AgCl electrode. The negative input to the amplifier was the signal from a separate reference Ag/AgCl electrode fed through a voltage follower utilizing another LH0042 operational amplifier. The positive input received an offset signal which was set under software control by the microcomputer utilizing its D/A converter. The working platinum electrode was connected to the chassis ground. A separate measuring platinum electrode was also present and used to read the solution potential vs. the reference electrode. This system maintained a voltage on the working platinum electrode, relative to the reference electrode, equal to the offset voltage that was set by the microcomputer. The program controlling the microcomputer adjusted the potential of the solution to the desired starting value. For an oxidative titration, the starting working voltage was set 200 mV above the starting solution potential, and, for a reductive titration, it was set 150 mV lower. Using a programmed series of pulses at the working voltage separated by brief pauses during which the working electrode was set at the same voltage as the solution, a desired incremental change in solution potential was achieved. The potential of the working electrode was then set to follow the measured potential of the solution for a period of 3 min to allow

equilibration of the redox components with the injected charge. After equilibration, a trigger pulse sent from the computer to the spectrometer caused the spectrum to be taken and stored in the spectrometer memory. The spectrometer memory was immediately transferred via the microcomputer to a floppy disc for storage and ultimate accumulation of all of the spectra of the experiment. After a desired voltage was achieved and the spectrum taken and stored, the working voltage was adjusted by an incremental amount to maintain sufficient oxidizing or reducing power with reference to the solution. The program was written to recognize when the voltage change in the solution was occurring too rapidly or too slowly and to take corrective measures by adjusting the working voltage and pulsing times to smooth out the titration curve. The maximum working voltage allowed was +400 mV relative to the reference Ag/AgCl electrode, which is +600 mV vs the normal hydrogen electrode. The accumulated spectra were then transferred through the microcomputer and a telephone modem to a DEC system-10 main frame computer for data analysis. Details about the microcomputer system and its link to the main frame computer have been previously described (Reddy and Hendler, 1983).

RESULTS

In agreement with the results found for the α absorption peak of cytochrome oxidase in mitochondria (Reddy et al., 1986), the analyses of both the Soret and α band absorbances of the pure enzyme show three Nernstian titrating species. As in the mitochondrial study, the strongest evidence for this comes from the SVD analysis. As previously discussed (Shrager and Hendler, 1982; Reddy and Hendler, 1983; Shrager and Hendler, 1986), this method resolves the composite difference spectra into fundamental spectra that are uniquely enriched or impoverished with respect to the individual titrating species that are present. In addition, the voltage titrations of individual fundamental spectra may produce slopes of either positive or negative sign. When a sign change of slope is encountered or when one titrating species out of a suspected two or more is isolated in the titration of a fundamental spectral component, the existence of separate titrating species can be firmly established. This kind of analysis conducted as described in the accompanying paper (Reddy et al., 1986) on the mitochondrial cytochrome oxidase showed that three rather than two Nernstian components were present and titrated in the range of 100 to 450 mV.

The presence of the three titrating species is further shown by the identification of three distinct difference spectra that go with each of the titrating species. The first indication of this comes from the difference spectra reconstructed from the SVD procedure. Knowing the midpoint potentials and the corresponding spectra deduced by SVD, it is possible to go directly to the raw spectral data and take difference spectra in the voltage ranges that were indicated by SVD. When this is done, it is seen that the spectral changes occurring in these three voltage ranges agree with the spectra reconstructed from the SVD analysis. Two examples of this are shown in Fig. 1 and Fig. 2. The complete SVD analyses of nine control experiments consisting of six reductive and three oxidative titrations fixed the Em values of the three titrating components at 196 ± 2.8, 260 ± 3.0, and 341 ± 4.5 mV with corresponding n values of 2, 2, and 1, respectively.

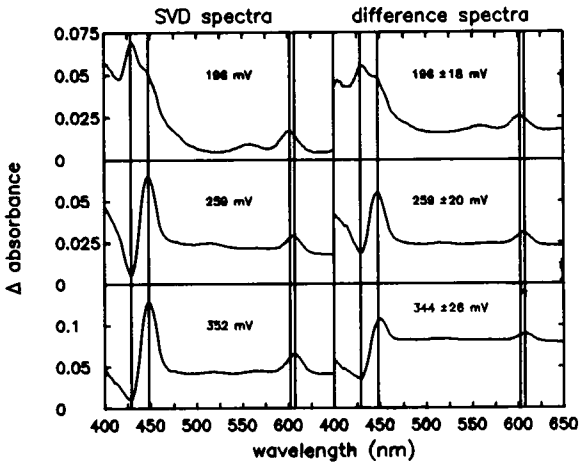

FIGURE 1 SVD-deduced difference spectra from experiment 132 listed in Table I are shown in the *left* hand panels. Corresponding difference spectra obtained from the raw data are shown for comparison in the panels to the *right*. The vertical lines in each panel are drawn at 429, 448, 602, and 607 nm.

An independent analysis of the titration behaviors of the individual α and Soret absorption peaks, using the second derivative method confirmed the presence of three Nernstian titrating components having the same Em values as deduced by the SVD procedure. When attempts were made to fit the experimental data to the traditional model using two components with Em values at 230 and 340 mV and n values of 1, much poorer fits were obtained in all cases (Table II). The problem which has posed the most difficulty is not whether three or two Nernstian species are present, but rather in the assignment of n values to the three Nernstian components that are present. The difficulty in this regard does not concern the component titrating at ~340 mV. Both SVD and the 2nd derivative analyses insist on an n = 1 for this component. Fits with

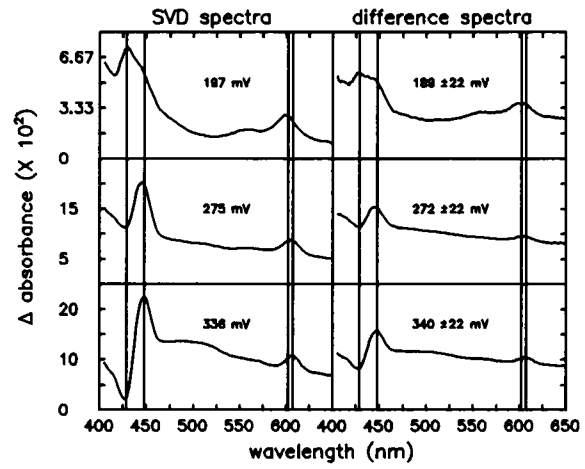

FIGURE 2 SVD-deduced difference spectra from experiment 153 listed in Table I are shown in the *left* hand panels. Corresponding difference spectra obtained from the raw data are shown for comparison in the panels to the *right*. The vertical lines in each panel are drawn at 429, 448, 602, and 607 nm.

TABLE II
SECOND DERIVATIVE AND SVD ANALYSES OF CONTROLS

n	604	447	429	SVD
	nm	*nm*	*nm*	
1	220 ± 6.8 (13)	225 ± 8.4 (10)	175 ± 10.7 (6)	202 ± 12.1 (4)
2	288 ± 7.7	261 ± 6.5	242 ± 2.3	275 ± 7.9
1	356 ± 5.1	338 ± 6.1	309 ± 4.0	332 ± 6.6
Rank	1.7 (13)	2.5 (13)	3.0 (6)	
2	187 ± 7.3 (13)	196 ± 13.4 (9)	177 ± 4.2 (6)	205 ± 5.2 (4)
1	266 ± 6.6	260 ± 7.0	260 ± 4.5	265 ± 11.8
1	356 ± 5.0	352 ± 8.3	327 ± 5.4	334 ± 6.3
Rank	2.0 (13)	2.2 (13)	2.0 (6)	
1	201 ± 10.4 (11)	177 ± 2.5 (3)	173 ± 8.8 (3)	202 ± 16.3 (3)
1	299 ± 8.5	253 ± 14.2	249 ± 5.0	269 ± 2.1
1	382 ± 7.8	337 ± 13.4	331 ± 4.2	338 ± 9.5
Rank	3.2 (13)	3.5 (13)	3.0 (6)	
2	193 ± 4.9 (13)	202 ± 6.1 (13)	173 ± 4.9 (6)	204 ± 5.9 (4)
2	262 ± 4.4	250 ± 4.9	249 ± 2.5	268 ± 2.6
1	342 ± 3.4	323 ± 5.7	314 ± 3.5	335 ± 3.3
Rank	3.8 (13)	2.2 (13)	2.0 (6)	
1	236 ± 5.9 (13)			
1	339 ± 3.8			
Rank	4.5 (13)			

The magnitude of the absorption peak was expressed in terms of the second derivative at the peak wavelength specified, as described in the methods and references. The voltage titration of each particular second derivative was analyzed according to models containing two or three Nernstian components with n values as shown. The analyses provided E_m values in millivolts for each component. The number of experiments shown in parenthesis alongside the low E_m component were analyzed to yield averages ± standard errors. The analysis was performed using a DEC-10 main frame computer and the MLAB program. For each experiment, the root mean square deviation error was used to rank the fits from 1 to 5 in terms of closeness of fit (1 is best). The average value of the ranking is shown, and based on this average for the analysis of the second derivative at 604 nm, the different models are arranged from best (*top*) to worst (*bottom*). In several cases the desired model could not be fit. In these cases, the model was not used for averaging the E_m values, but it was given a rank of 5 and used for averaging the quality of the fit. This is why in some cases, the number of experiments used for E_m values is seen to be lower than the number shown for the "Rank." Independent analyses of the same models with SVD were also performed and the E_m values obtained by this procedure are also shown.

$n = 2$ are not possible or are very poor. For the component titrating at 200 mV, SVD strongly indicates $n = 2$, whereas the 2nd derivative procedure applied to the α absorption peak provides fits with lower root mean square deviation errors with both the 2,1,1 and 1,2,1 models than with a 2,2,1 model (Table II). This ambiguity regarding the n value for the first (~200 mV) component becomes more pronounced in regard to the second (~260 mV) component. This is because certain of the SVD titration curves can be fit with an $n = 1$ value for this component.

A variety of different analytical procedures have been used to obtain a more clear-cut resolution of the n values for the two lower E_m components that are present. The criterion used is that the true model should prevail in its consistency with all of the different methods used. Rather then just using root mean square deviations for judging fits, values of dependency[1] and standard errors for each fitted parameter were considered. The different methods used were: (a) Second derivative analysis at 604 nm; (b) Second derivative analysis at 447.5 nm; (c) Second derivative analysis at 429 nm; (d) SVD analysis.

With the third (i.e. 340 mV) component fixed at $n = 1$, there are four models to choose from, namely, 1,1,1; 2,1,1; 1,2,1; and 2,2,1. The ranking for fits using these models based on the root mean square deviation error in the fittings of the α peak, as the criterion for judging the fit, place the models in order of best to worst as 1,2,1; 2,1,1; 1,1,1; and 2,2,1 (Table II). Using the principal Soret band (447.5 nm) for the 2nd derivative procedure, the 2,2,1; and 2,1,1 models come out somewhat better than the 1,2,1 model and the 1,1,1 model does most poorly. Clearly, the root-mean-square deviation is not a sufficient means for resolving the problem.

Other indications of the quality of the fits using 2nd derivative data were available. That is, in many cases, poor models led to fits, but the dependency values approached or reached the limit of 1.000000 and the standard errors approached $\pm\infty$. Sometimes, the fit for the amount of a reduced minus oxidized peak returned a negative number whereas these characteristic features are known to be positive (i.e., they appear upon reduction). In other cases a fit initialized for a particular model such as 2,1,1 inverted the fitted E_m parameters so that a 1,2,1 fit was returned. This also happened in reverse where an attempted 1,2,1 fit returned a 2,1,1 fit. The only model which did not run into any of these problems was the 2,2,1 model.

The SVD analytical procedure was also used to resolve the question of n values for the two lower E_m components. Although when using this procedure and attempting to achieve the best fits for the titrations of the fundamental spectra we arrived at the 2,2,1 model, it was decided to obtain fits, forced if necessary, that would be consistent with each of the other three models. This was done by imposing the n value for the first or second component as specified by the model. Four titration experiments were examined in this way (Table III). Two (No. 151 and No. 153) used spectral information covering both the Soret and α regions, and two (No. 79 and No. 80) used spectral information restricted to the α region. For the complete spectral range, one was an oxidative titration (No. 151) and the other a reductive titration (No. 153). The E_m

[1]High dependency of a given parameter on the value of another means that more than the essential minimum number of parameters have been used. This indicator of "goodness of fit" is further discussed by Shrager and Hendler, 1986, and Reddy and Hendler, 1983.

TABLE III
TEST OF DIFFERENT MODELS BY SVD

EXP.	2,2,1 SVD	2,2,1 2nd D	2,1,1 SVD	2,1,1 2nd D	1,2,1 SVD	1,2,1 2nd D	1,1,1 SVD	1,1,1 2nd D
	192	215	(199)	214	181	239	(195)	233
151	268	274	(284) **	285	(269)	325	(272) *	333
	326	349	348	363	327	379	248	403
								+
	197	195	(194)	194	(181)	214	(178)	201
153	275	278	(259)	306	(295)	306	(265)	320
	336	351	320	371	317	363	319	384
	214	169	213	147	(223)	189		
79							Fits too poor to allow reconstruction	
	263	247	234	254	258	256		
	337	330	340	349	348	336		
			+					
	215	220	215	219	223		(233)	
80	265	269	(283) *	261	(280)	No Fit	(270)	No Fit
	342	350	327	356	(336)		347	
			+		+		+	

The models tested are referred to by the n values listed in sequence for the E_m species in the order of 200 mV, 260 mV, and 340 mV. Thus 2,2,1 is for the 200 and 260 mV species, both with $n = 2$ and the 340 mV species with $n = 1$. The numbers in the table are in groups of three and represent E_m values listed from low to high, obtained for the titrating species by either the SVD method or the second derivative method centered at 604 nm. In testing a particular model, the n values are fixed as specified by the model. Three kinds of failure are shown in the table. An "*" shows when the titration was present but could not be fit by the imposed n value. A double "*" indicates that this failure occurred in the titrations of two of the fundamental spectra. An "+" shows where the fit using the imposed n values had dependency values[1] at or very near the limit of 1.00000 for one or more of the three Nernstian species. This means that an independently titrating species is not seen in the model tested. SVD allows the reconstruction of the difference spectrum for each titration transition it finds. A verification of the reliability of the SVD analysis is obtained when the actual difference spectrum taken from the raw data around the voltage indicated by the SVD determined E_m, shows similarity to the SVD-deduced spectrum. When little or no correspondence is seen between the actual and SVD-deduced spectra for an SVD determined E_m, the validity of the SVD treatment must be doubted. Correspondingly, agreement between the spectra provides support for the SVD analysis. The circled values in the table show where little or no agreement was seen between the two spectra for the indicated SVD solution.

values obtained in each experiment for each model by the SVD procedure are shown in comparison to the E_m values obtained for the same model using the 2nd derivative procedure centered at 604 nm. The forced fits using the models 2,1,1; 1,2,1; and 1,1,1 displayed three kinds of failures. In some cases when an $n = 1$ was tried for the transition occurring at 250 mV, the fit was not successful as judged by the wide discrepancy between the data and fitted curve for the component. This failure is shown as an "*" in the table. In some cases, reasonably good fits were obtained but the dependency values for one or more of the three titrating species were at or very near the limit of 1.00000. This indicates that a unique titrating species of the kind sought was not present and that the fit of the component was dependent on the fit applied to another component used in the fitting procedure. This failure is shown as a "+" in the table. A third kind of failure is seen when the reconstructed spectrum obtained by the SVD procedure for a particular titrating species shows little or no resemblence to the actual difference spectrum taken in a range of about ±20 mV of the indicated E_m value. This failure is shown as a circle around the fitted E_m value for the component. The only model that passed all of the tests is seen to be the 2,2,1 model. The results obtained with this model are consistent with the results obtained by the 2nd derivative procedure applied to all α and Soret absorption peaks, are also consistent with actual difference spectra and correspond to the conclusions reached by a similar analysis using the α peak absorbance of the enzyme in situ in the mitochondria (Reddy et al., 1986).

As shown in Figs. 1 and 2, and in virtually all similar experiments the three titrating species have peak α absorbances at 602, 605, and 607 nm, respectively, for the 200, 260, and 340 mV forms. The Soret peak absorbances for the same three species were at 429, 446, and 448 nm. We would now like to point out that the absorbance at 429 nm

is representative of a labile form of the enzyme. It is seen only during a reductive titration and only when the titration is performed in the presence of a stabilizer. In order to protect the highly purified enzyme from possible denaturation by surface effects or by contact with the working platinum electrode and to provide lipoprotein components, we have added a mixture of egg proteins and lipids in the form of a total egg homogenate at a concentration of 5 mg protein per ml. All reductive titrations performed in the presence of the egg homogenate show the predominent Soret absorbance for the 200 mV component at 429 nm. This is seen both in the SVD reconstructed spectrum for this component and in direct difference spectra taken in a narrow voltage region around the value of the E_m determined for this species by SVD. It is also seen in the 2nd derivative analysis at 429 mV. A representative spectrum for this titrating species is shown in Fig. 3 (solid line, top panel). In an oxidative titration ± egg homogenate, this species is virtually absent and the spectral change occurring in the Soret region is at 447 nm (solid line, bottom panel). A reductive titration performed in the absence of egg homogenate shows the absorbance somewhere between the 429 and 447 nm extremes (dashed line, top panel). This figure shows spectra from four different experiments. A dramatic confirmation of this phenomenon is seen in a "turn around" experiment. The sample is first reductively titrated to about 95 mV and then immediately retitrated in an oxidative direction. When egg homogenate was present, the major Soret absorbance was seen at 427 nm, Fig. 4

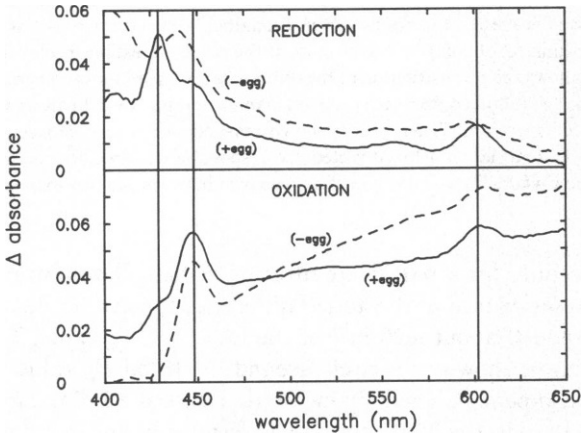

FIGURE 3 Conditions for the appearance of the spectrum of the low E_m component with a Soret peak at 429 nm. The *top* panel shows the difference spectrum obtained at 175 ± 22 mV in experiment 133 (solid line) which was a reductive titration performed in the presence of 15 mg protein of an egg homogenate. The dashed line in the same panel is a difference spectrum obtained at 177 ± 22 mV in experiment 154 which was a reductive titration performed in the absence of the egg homogenate. The *lower* panel shows two difference spectra obtained in oxidative titrations. The solid line was obtained at 187 ± 20 mV in experiment 145 performed in the presence of the egg homogenate and the dashed line was obtained at 176 ± 21 mV in experiment 151 performed in the absence of egg homogenate. The peak at 429 nm is seen only in reductive titrations performed in the presence of the egg homogenate. The vertical lines are drawn at 429, 448, and 602 nm.

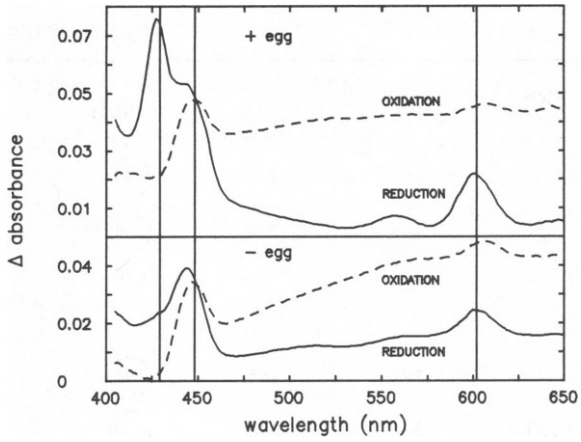

FIGURE 4 Reductive and oxidative titrations performed in the same experiment. The *top* panel shows the difference spectrum obtained at 173 ± 17 mV during a reductive titration in experiment 152 performed in the presence of 15 mg protein of hen homogenate (solid line). The dashed line shows the difference spectrum obtained at 183 ± 22 mV during an ensuing oxidative titration performed on the same sample. The *bottom* panel shows an analogous experiment performed in the absence of egg homogenate. The difference spectrum obtained at 178 ± 22 mV during the reductive phase is the solid line and the difference spectrum obtained at 180 ± 21 mV during the oxidative phase is the dashed line. The vertical lines are drawn at 429, 448, and 602 nm.

(solid line, top panel). The ensuing oxidative titration showed the Soret peak at 447 nm (dashed line, top panel). In the absence of egg homogenate, the Soret peak in the reductive titration was at 443 nm (solid line, bottom panel). The ensuing oxidative titration showed the Soret peak at 447 nm (dashed line, bottom panel). Both reductive titrations performed in the presence of egg homogenate show a hump at 447 nm on the major Soret peak at 429 nm (Figs. 3 and 4, top panels, solid lines). These humps could be due to the tailing of the titrations of the 260 mV species, or to some kind of equilibrium between two spectral forms (conformations) of the 200 mV species. An indication that two forms of the low voltage species exist is seen in the relative amounts of all titrating species as fixed by the 2nd derivative analyses at 447.5 nm. In the oxidative titrations the three Nernstian species are present in the relative amounts of 0.3206 ± 0.0597, 0.3781 ± 0.0812, and 1.0571 ± 0.1948 respectively for the 200, 260, and 340 mV species. In the reductive titrations (+egg), analyzed at 447.5 nm, the relative amounts were 0.1479 ± 0.0280, 0.3265 ± 0.0470, and 0.9517 ± 0.0884. There were no apparent changes in the amounts of the middle and high voltage species, but the amount of the 200 mV species appears to have been reduced by ~50%. Titrations of egg homogenate plus mediators in the absence of cytochrome oxidase showed none of the effects that have been discussed above.

The difference spectrum of the 200 mV component with a Soret peak at 429 nm and an α peak at 602 nm is quite similar, if not identical, to that of a form of cytochrome oxidase first described by Okunuki et al., in 1957. This

species was formed by treating freshly reduced enzyme with oxygen. It is known today as the oxygenated or pulsed form of cytochrome oxidase. Much research over the years has shown that this form of the enzyme is kinetically more competent than the resting enzyme in catalyzing the oxidation of reduced cytochrome *c*. This form of the enzyme is labile and decays on a time scale measured in minutes. In this respect, it also resembles the species of cytochrome responsible for the spectral change we have observed. More recently it has been shown that the same spectrum can be generated by treating the oxidized enzyme with H_2O_2 and it is suggested that the spectrum is that of a peroxide complex of the enzyme (Kumar et al., 1984). We first saw this spectrum in an anaerobic reductive titration of the oxidase using $Na_2S_2O_4$. It seemed possible that enough H_2O_2 may have been generated during the oxidation of the dithionite to allow the formation of such a complex. We, therefore, performed an electrical reductive titration in which no dithionite was present. Fig. 5 shows that the same spectral change was observed during the titration of this component. In fact, an electrical titration performed in the presence of 50 nM catalase (697 units/ml) did not eliminate this spectral species (Fig. 5). The addition of 1 mM H_2O_2 to the titration system did not augment the spectral change. These experiments show that the spectrum is not uniquely explained as a peroxide derivative of cytochrome oxidase.

The effects of pH and ligands on the E_m values of three Nernstian components in the 2,2,1 model were examined with the 2nd derivative method at 604 nm and with the SVD method (Table IV). Raising the pH one unit to 8.0 caused a decrease of ~30 mV in the E_m values of all three species. Lowering the pH one unit to 6.0 showed a corresponding rise of about 30 mV for all three species analyzed by the 2nd derivative procedure. SVD, however, confirmed the effect for the high voltage component but not for the two lower E_m components. Neither azide nor cyanide showed significant effects on the E_m values of any of the three components. In two experiments in which the enzyme was preincubated 20 h at 4°C with cyanide prior to the titration, a new titrating species was seen with $E_m = 227 \pm 2.0$ mV and $n = 2$. The effect of carbon monoxide was quite pronounced. The E_m values of the middle and high voltage components were both decreased by 20 to 30 mV. The 200 mV component with Soret peak at 429 nm and α peak at 602 nm was no longer evident. In its place were seen two new components, both possessing the spectral characteristics long associated with the carbon monoxide adduct of cytochrome oxidase. This spectrum has a Soret peak at ~435 nm and an α peak at ~594 nm. Fig. 6 shows the spectra for the four Nernstian components present in the carbon monoxide titrations. Both SVD deduced and actual difference spectra are shown. The E_m values for the two characteristically carbon monoxide complexed forms were unambiguiously fixed by SVD, and second derivative analyses at both the 435 and 594 nm peaks at about 115 and 205 mV (Table IV). This finding supports independent observations based on IR stretching modes that two major species of CO adduct to the bovine cytochrome oxidase exist (Yoshikawa and Caughey, 1982). The SVD procedure found $n = 4$ for the 205 mV species, but it could not decide between $n = 1$ or $n = 2$ for the species titrating near 115 mV. These direct determinations of the E_m values of the carbon monoxide complexed species are in direct opposition to the view, long held, that the carbon monox-

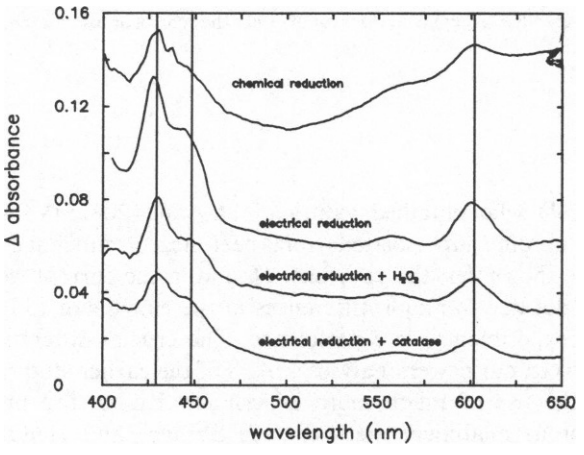

FIGURE 5 Appearance of the Soret peak at 429 nm in difference spectra from reductive experiments in the presence and absence of peroxide and catalase. All reductive experiments were performed in the presence of 15 mg of protein of chicken egg homogenate. The *top* curve was obtained at 179 ± 22 mV in experiment 128 which was a chemical reduction. The *next lower* curve was obtained at 172 ± 23 mV in experiment 152 which was an electrical reduction. The *next lower* curve was obtained at 175 ± 22 mV in experiment 133 which was an electrical reduction performed in the presence of 1 mM H_2O_2. The *lowest* curve was obtained at 186 ± 21 mV in experiment 132 which was an electrical reduction performed in the presence of 50 nM catalase (697 units/ml). The vertical lines are drawn at 429, 448, and 602 nm.

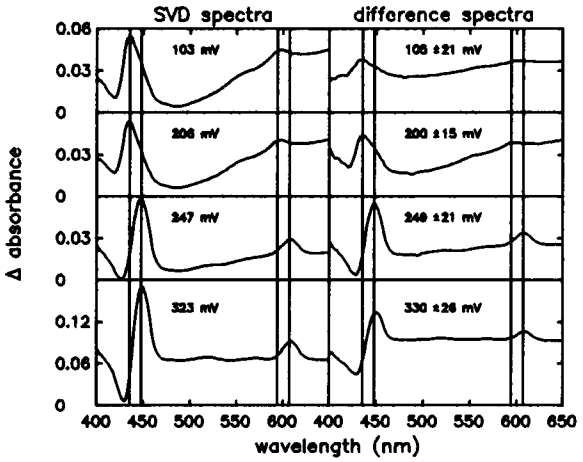

FIGURE 6 SVD-deduced difference spectra from a chemical reduction (EXP. 130, Table I) performed under a carbon monoxide atmosphere are shown on the *left*. Corresponding difference spectra obtained from the raw data are shown in the panels on the *right*. The vertical lines are drawn at 435, 448, 594, and 607 nm.

TABLE IV
EFFECTS OF pH AND LIGANDS ON E_m VALUES

CONDITION	n	E_m Values mV		Change From Control mV	
		2nd Derivative	SVD	2nd Derivative	SVD
Control	2	193 ± 4.9	196 ± 2.3		
	2	262 ± 4.4	260 ± 2.7		
	1	342 ± 3.4	340 ± 4.8		
		(13)	(10)		
pH 8.0	2	160 ± 1.0	172 ± 2.1	−32	−24
	2	232 ± 4.0	235 ± 8.0	−30	−25
	1	307 ± 2.0	304 ± 2.0	−35	−36
		(2)	(2)		
pH 6.0	2	217 ± 5.0	197 ± 2.0	+24	—
	2	290 ± 1.0	265 ± 1.0	+28	+5
	1	377 ± 11.0	367 ± 5.5	+35	+27
		(2)	(2)		
Cyanide (1 mM)	2	203 ± 8.9	195 ± 5.0	—	—
	2	267 ± 6.4	264 ± 4.0	—	—
	1	347 ± 7.5	342 ± 8.4	—	—
		(5)	(5)		
Azide (10 mM)	2	200 ± 8.3	196 ± 4.8	—	—
	2	269 ± 6.1	259 ± 3.8	—	—
	1	351 ± 5.8	340 ± 7.2	—	—
	*	(8)	(7)		
Carbon monoxide	1 or 2	128 ± 15	105 ± 2	No comparison	No comparison
	4*	207 ± 2	208 ± 2		
	2	236 ± 5	243 ± 3	−26	−17
	1	305 ± 2	320 ± 3	−37	−20
		(2)	(2)		

The average E_m ± standard error is given for the number of experiments shown in parentheses. Data are given for both the second derivative analysis at 604 nm (unless otherwise noted) and for the SVD analyses. Changes which are less than the larger standard error of either the control or tested condition are not listed separately.

*594 nm. The same results were obtained with the second derivative analysis at 435 nm.

ide-liganded form must possess a greatly elevated E_m value compared to the uncomplexed enzyme. This point will be considered in some detail in the Discussion.

Fig. 7 is presented as a bridge between our studies and previous thermodynamic analyses of isolated cytochrome aa_3. One of the electrical reductions performed with the enzyme was analyzed by the same two-point ΔA graphic method in common usage during the past 15 years. The sigmoid on the left was obtained by plotting E vs. the apparent log (oxidized/reduced) determined from the ΔA between 605 and 626 nm. The two lines drawn at the extremes are theoretical $n = 1$ curves. The panel on the right was derived from the data on the left by the graphic analyses technique of Wilson and Dutton (1970, and personal communication with these authors). The two "resolved" curves show some small scatter around two theoretical $n = 1$ curves with E_m values of 353 and 213 mV. This may be compared to Figs. 2 and 3 of Leigh et al. (1974) who obtained values of 360 and 208 mV with cytochrome aa_3 isolated from beef heart mitochondria. This shows that the differences found in the current work are not due to major differences in the enzyme or to how the experiments were performed. The crucial differences between our newer analyses and all of the earlier studies is in the use of much more experimental data and more rigorous analytical methods (see Shrager and Hendler, 1986).

Direct Demonstration of the Presence of Two $n = 2$ Components Rather Than One $n = 1$ Component

The existing view of the Nernstian properties of cytochrome oxidase is that two species are present, one with E_m ~340 mV and the other with E_m ~230 mV. Both species have an n value of 1 (see Wikström et al., 1981). The

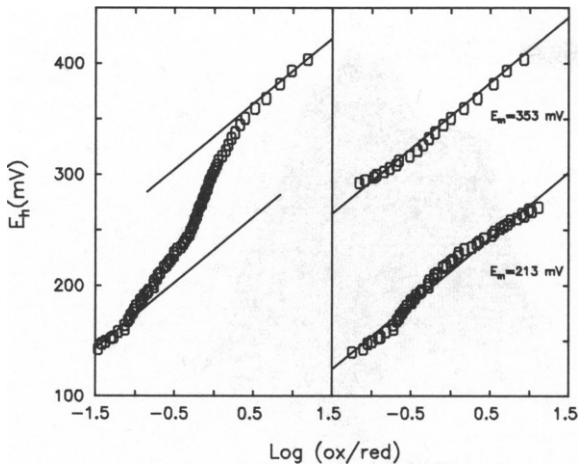

FIGURE 7 An electrical reduction experiment using pure cytochrome aa_3 and a spectral range concentrated in the α absorbance region (Exp. 80, Table I, accompanying paper) was analyzed using the ΔA between 605 and 626 nm as the measure of reduction. The panel on the left used the ΔA observed in the experiment. The two lines drawn at the extremes are theoretical $n = 1$ curves. The panel on the *right* shows the resolution of the data on the *left* into two components with slopes very close to the theoretical $n = 1$ lines that are shown and E_m values of 363 and 213 mV. The resolution technique is that of Wilson and Dutton (1970, and personal communication).

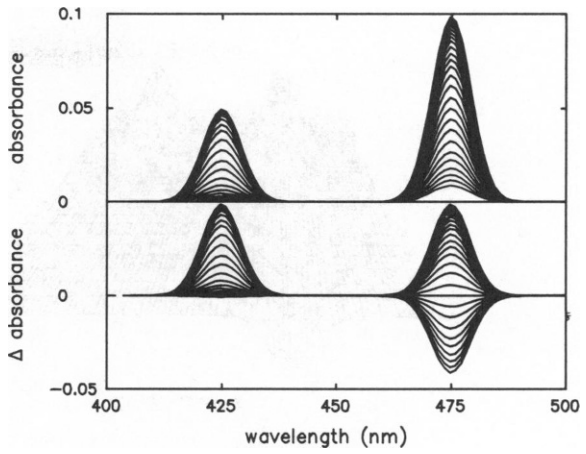

FIGURE 8 (*a*) *top* panel, *left* side; Computer simulated titration of a Guassian shaped absorption feature with a maximum ammplitude of 0.05, an E_m of 175 mV, n value of 2, peak centered at 425 nm, half width of 5 nm and voltages as obtained in exp 152 (reduction) of Table I (right side). Computer simulated titration of a Guassian feature with a maximum amplitude of 0.1, an E_m of 230 mV, n value of 1, peak centered at 475 nm, half width of 5 nm and voltages as obtained in exp. 152 (reduction) of Table I. (*b*) *bottom* panel: Difference spectra generated from the spectra shown in *top* panel, formed by subtracting the spectrum at 230 mV from all of the other spectra in each of the two cases.

conclusions reached in the current investigation confirm the presence of an $n = 1$ component with E_m ~340 mV but disagree on the existence of an $n = 1$ component with E_m ~230 mV. The apparent $n = 1$ component is resolved into two $n = 2$ components, or rather an $n = 2$ component with another $n = 2$ component that forms an equilibrium distribution among two species with Soret maximums at 429 and 448 nm. The average E_m value for the species with a Soret maximum at 429 nm is 173 ± 4.9 mV and the average E_m for the other is 202 ± 6.1 mV (Table III). The conclusions reached in the current work are based on two different methods which involve computer analysis. However, it is possible with no computer analysis to demonstrate the essential correctness of the conclusions from the original unprocessed data. The major question to be resolved is whether a single species with E_m ~230 mV and $n = 1$ is present, or whether the mixture we have defined is present. To decide this question, both models were constructed using a theoretical Gaussian shape to represent the optical absorbance feature and basing the size of the Gaussian at each voltage on the Nernst equation. In one case an E_m of 230 mV, an n value of 1, and a total amount of 0.1 was assigned. In the other case, an E_m of 175, an n value of 2, and a total amount of 0.05 was assigned. The actual voltages and wavelengths of experiment 152 (Table I) were used for computing the size of the Gaussians and for plotting. The two sets of Gaussians were arbitrarily centered at 425 and 475 nm for pictorial display (Fig. 8, top). A reference spectrum at 230 mV was used to generate difference spectra from the two sets of Gaussians (Fig. 8, bottom). A clear difference is seen between the two models. The difference spectra in the $n = 1$ case with E_m = 230 mV are symmetrically distributed around the central curve at 230 mV, whereas in the $n = 2$ case with E_m = 175 mV, they are almost entirely above (i.e. on the reduced side) of the reference spectrum at 230 mV. The difference between the two cases is more dramatically seen in the three-dimensional plot of Fig. 9 (left side) where the perspective of voltage has been added. This view, which is from the high voltage side, places the $n = 2$ case on the right. The single $n = 1$ model shows a positive rise above the plane on the low voltage side, a descent to plane level at 230 mV and a smooth descent into a valley on the high voltage side. A line running across the crest and down into the trough describes the Nernstian sigmoid of a plot of the amount reduced vs. voltage. The height of the "mountain" and the depth of the "valley" are exactly symmetrical at equivalent voltages away from the central value of 230 mV in the $n = 1$ case. The $n = 2$ case with E_m at 175 mV shows a more rapid descent of the "mountain" on the low voltage side to the plain beginning at 230 mV and no depression below the surface at the higher voltages. Fig. 9 (right side) shows the actual raw data of experiment 152. The valley in the foreground at 447 nm is complemented by a mountain on the low voltage side of 230 mV. This could be due either to a single $n = 1$ species with E_m at 230 mV or to two $n = 2$ species with E_m values at about 200 and 260 mV. The absorbance trough at 447 nm on the high voltage side rises to a peak at ~429 nm. Both the trough at 447 and the peak at 429 nm are features of the spectrum of the species being titrated in this voltage range. That the species is not an $n =$

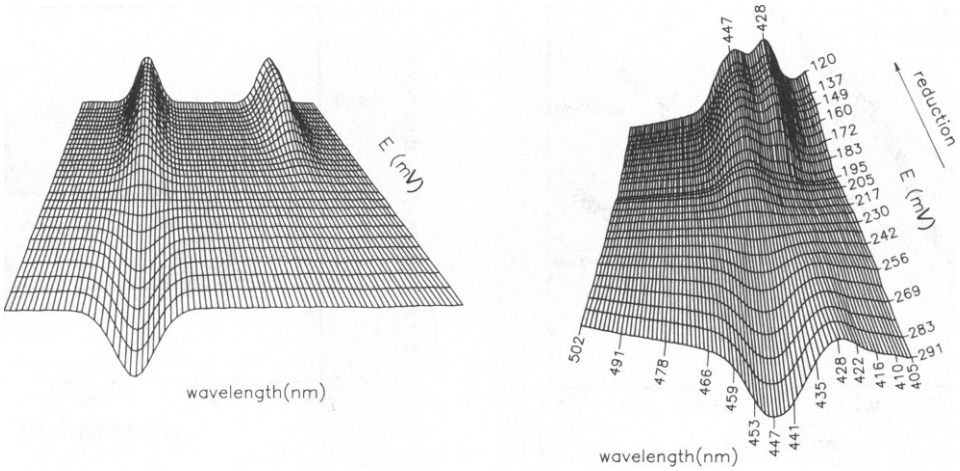

FIGURE 9 *left side:* three-dimensional representation of the spectra shown in Fig. 8 *b*. The view is from the high voltage side looking in the direction of lower voltages. The grid is identical to the one shown on the *right side* with respect to wavelength and voltage lines. The wavelength grid from *left to right* is from 501.6 nm to 405.2 nm with a spacing of 1.23 nm. Wavelengths are shown to the nearest whole number. The $n = 1$ Guassian is on the *left* and the $n = 2$ Guassian on the *right* in this view of the surface. (*right* side) three-dimensional representation of exp 152 (reduction). The orientation is as described for the *left* panel surface. As discussed in the text, this figure shows the presence of two $n = 2$ components with E_m values on both sides of the 230 mV reference rather than a single $n = 1$ component with E_m value at 230 mV.

1 with E_m at 230 mV is shown by the fact that instead of a symmetrical valley at 429 nm on the low voltage side, there is another mountain at this wavelength. This absorbance maximum at 429 nm is uniquely characteristic of the low voltage component that we have identified with an E_m 175 mV and an n value of 2. The characteristics of the feature centered at 429 mV are totally inconsistent with the existence of a single $n = 1$ species with E_m at 230 mV and entirely in agreement with the presence of two separate species with n values of 2 and E_m values on both sides of the 230 mV dividing line. Fig. 10 shows a surface from an oxidative experiment performed in the absence of egg homogenate (exp. 150, Table I). This surface shows that the labile species with E_m ~175 mV and Soret maximum at 429 is not present under the conditions of this titration, as discussed above (see Figs. 3 and 4).

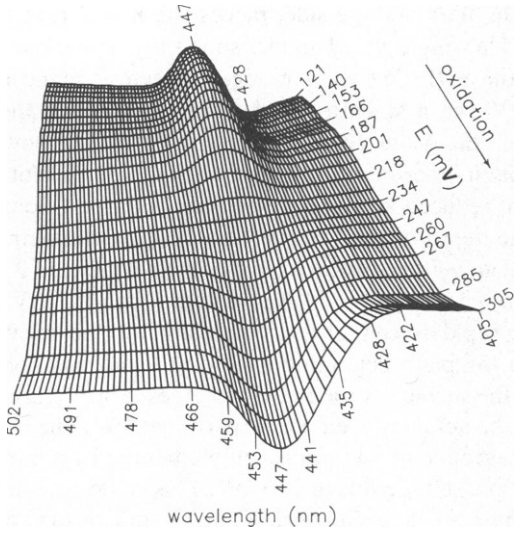

FIGURE 10 Three-dimensional representation of exp. 150 (oxidation). The orientation is as described in Fig. 9. This surface compared to Fig. 9 (*right*) shows the absence of the labile species responsible for the Soret absorption at 428 nm, which is seen only upon reductive titrations in the presence of egg homogenate.

DISCUSSION

In an accompanying paper (Reddy et al., 1986), it is shown that the α absorbance feature of cytochrome oxidase in situ in beef heart mitochondria displays three distinct Nernstian titrations. One has an E_m of ~190 mV, a difference peak centered at 602 nm and an n value of 2; another has an E_m of ~260 mV, a peak centered at 605 nm and an n value of 2; and the other has an E_m of ~340 nm, a peak centered at 607 nm and an n value of 1. These values were arrived at in a combination of ways that utilized analyses by the second derivative technique and the procedure of singular value decomposition and confirmations obtained by taking difference spectra across restricted voltage regions on both sides of the deduced E_m values. It was shown that traditional methods which utilize a two-point ΔA method of data collection and a graphical method of analysis are incapable of resolving the mixture of Nernstian components which are present (Reddy et al., 1986; Shrager and Hendler, 1986). In the present work, purified cytochrome oxidase was used and the analyses were broadened to include the Soret absorption peaks as well as the α absorption peaks. The findings with respect to the α absorption features confirm the findings obtained with the intact mitochondria. As a result of the current work we are now able to describe the complete optical difference spectrum of each of the three Nernstian components of cyto-

chrome oxidase by adding a unique Soret feature to each of the α peaks that have been characterized. Thus, the component with E_m at ~190 mV, n value of 2, and α peak at 602 nm, has a Soret peak at 429 nm; the component with E_m at ~260 mV, n value of 2, and α peak at 605 nm, has a Soret peak at 446 nm; and the component with E_m at ~340 nm, n value of 1, and α peak at 607 nm, has a Soret at 448 nm. The existence of each of the three Nernstian species was confirmed by separate analyses based on the 2nd derivative analyses of the Soret peak, the 2nd derivative analysis of the α peak, the SVD analyses of either the entire spectrum or the isolated α absorption region, and difference spectra taken around the three E_m positions.

Titrations under an atmosphere of carbon monoxide were used to characterize the cytochrome a_3 components. It has long been known that the characteristic absorption spectrum of the carbon monoxide adjuct of cytochrome a_3 has an α peak near 594 nm and a Soret peak near 435 nm. We have found that under a carbon monoxide atmosphere, the characteristic carbon monoxide altered spectrum was seen at the expense of the spectrum with α peak at 602 nm and Soret peak at 429 nm, which was absent from these titrations. This component with E_m at ~190 mV is the same one identified as cytochrome a_3 in the experiments carried out with the intact mitochondria (Reddy et al., 1986). As in the studies with mitochondria, we find that the major Nernstian transition of the characteristic liganded species has a nonelevated E_m value and an n value higher than 1. A minor species of the liganded form displays a lowered E_m value. Thus, as in the accompanying study, we disagree with Wilson et al. (1972), on the identification of cytochrome a_3, which we see as a low voltage rather than a high voltage form of cytochrome oxidase. We also fail to confirm the widely believed concept, that liganding the reduced form of cytochrome a_3 to carbon monoxide must lead to an increase in its E_m. We have shown in an accompanying paper (Reddy et al., 1986), that theory does not require that the E_m be raised, if redox-related proton dissociations occur on the liganded cytochrome oxidase and that our findings are not in conflict with other experimental data on the Nernstian characteristics of cytochrome oxidase in the presence of carbon monoxide during mediated anaerobic titrations. On the other hand, we do not dispute the conclusion that the liganding of cytochrome a_3 to carbon monoxide, followed by oxidation of the enzyme does appear to "lock" heme a_3 in a reduced state. Our analysis of these apparent discrepant observations suggests the possibility that the E_m of cytochrome a_3 is regulated by the redox state of one of the other redox centers present (Reddy et al., 1986). This idea finds strong experimental support from the data itself. Consider that, when all of the other centers are oxidized, the redox potential of cytochrome a_3 is raised above that of $K_3Fe(CN)_6$ (E_m = 420 mV). However, when the other centers become reduced, the redox potential of cytochrome a_3 falls to the value we have determined (E_m = 190 mV). This means that the reduced spectrum with its prominent Soret absorption at 429 mV will disappear as the other centers are reductively titrated due to the sudden drop in redox potential and resulting prompt oxidation of cytochrome a_3. The appearance of the reduced form of the Soret band for the other center then should be accompanied by the disappearance of the Soret peak at 429 nm. The newly formed, oxidized, low potential cytochrome a_3 will then be reduced as the voltage is progressively lowered, resulting in a new growth of the Soret peak at 429 nm as the reducting titration is continued. *This is exactly what does happen.* Figs. 1 and 2 show both actual difference spectra and SVD reconstructed spectra for two reductive titrations. It is seen that the appearance of the characteristic Soret absorptions for the two other titrations centered with E_m values at 340 and 260 mV are accompanied by a distinct inverted Soret peak at 429 nm. As the titration is then continued to lower voltages, the prominent Soret peak at 429 nm reappears.

This newly formed low potential species of cytochrome a_3 is labile and requires stabilization afforded by a mixture of proteins and lipids present in a homogenate of whole chicken egg. Furthermore, it is not seen during an oxidative titration, even during the same experiment when a reductive titration is immediately followed by an oxidative titration. Both in its optical spectrum and its lability, this form of cytochrome oxidase strongly resembles the pulsed or oxygenated form of the enzyme that has been known during the last 28 years (Okunuki et al., 1957; Kumar et al., 1984). This form of the enzyme is made by first reducing cytochrome oxidase and then pulsing with oxygen or simply oxidizing with a chemical oxidant and exposing the enzyme to peroxide. The Soret peak at near 429 nm and α peak near 602 nm are characteristic of this species as well as its lability. The pulsed form has a higher kinetic capability for catalyzing the oxidation of cytochrome c by oxygen. Both the characteristic spectral features and enhanced catalytic abilities decay on a time scale measured in minutes. We believe, therefore, that the thermodynamic species characterized in our work as cytochrome a_3 is most likely related to the pulsed form of cytochrome oxidase (see Reddy et al., 1986). If this is true, then either the elevated redox potential of heme a_3 is close to that of oxygen, or the conformational state of the enzyme is such that the reduction of bound O_2 by heme a_3 is not effected at this stage.

A discussion of the thermodynamic behavior of cytochrome oxidase must include a consideration of possible cooperative interactions between the various redox centers that are present (Malmström, 1974; Nicholls and Petersen, 1974). This is appropriate because the enzyme must accommodate four electrons in some order to effect the reduction of oxygen to water. A specific form of cooperativity has been invoked to reconcile the two transition model of Wilson et al. (1972) with seemingly contradictory

data obtained from the effects of ligands for cytochrome a_3 on the absorbance feature centered near 605 nm (see Caughey, 1967; Lemberg, 1969; Wikström et al., 1976; Reddy and Hendler, 1986). This form of cooperativity (the "neoclassical" model) is entirely inappropriate for the three-transition model described in the present work. The model supported by the data in this paper does involve a form of cooperativity in which the redox state of heme *a* governs the E_m of heme a_3, but electrons acquired by one heme center are not considered to be shared with the other, and there is no need to explain the dilemma of how an absorbance feature supposedly due almost entirely to heme *a* titrates as 50% due to heme a_3 (see Wikström et al., 1981).

Our combined studies of the *b*, c_1, and *a* type cytochromes (Reddy and Hendler, 1983; Reddy and Hendler, 1986; Reddy et al., 1986; this paper) have shown consistent evidence for $n = 2$ stages of electron transfer. As previously mentioned (Reddy and Hendler, 1986) this is consistent with the facts that two electrons are removed from a substrate being oxidized and two electrons are required to reduce an atom of oxygen. The unfavorable thermodynamic aspects of a one-electron reduction of oxygen have long been considered as an argument in favor of some kind of concerted reduction of the molecule. Since individual heme groups can accommodate only one electron, achievement of a thermodynamic *n* value of 2 requires the tight coupling of two one-electron centers. In this connection it is worth noting that evidence exists for the dimeric character of both the b-c_1 complex and cytochrome oxidase (Rieske and Ho, 1985; Georgevich et al., 1983).

The effects of pH and the presence of various ligands on the titration behavior of the pure enzyme were studied and the results are summarized in Table IV. It appears that the E_m of all three Nernstian components decreased ~30 mV upon a pH change from 7 to 8. The high voltage component increased ~30 mV on decreasing the pH from 7 to 6. The middle and low voltage component also increased, but the extents of the increase may be <30 mV. Similar but not identical effects were seen with the enzyme in situ in the mitochondria (Reddy et al., 1986). No effects on the titration characteristics were seen in the presence of cyanide or azide, although these agents did provoke small decreases in E_m in the mitochondrial-associated enzyme and azide did cause profound general changes in the absorption spectrum of the mitochondrial system (Reddy et al., 1986).

A discussion of the possible significance of *n* values of 2, 2, and 1 and of mole fractions of the three individual Nernstian components is given in the accompanying paper (Reddy et al., 1986).

Although we would prefer simply to present the data and not speculate on models, we feel obligated, in view of the unexpected nature of our findings, to show how the newer aspects of the current work could be accommodated in terms of current knowledge of cytochrome oxidase. A possible explanation of the 2,2, and 1, *n* values seen in the titrations is represented by the following scheme.

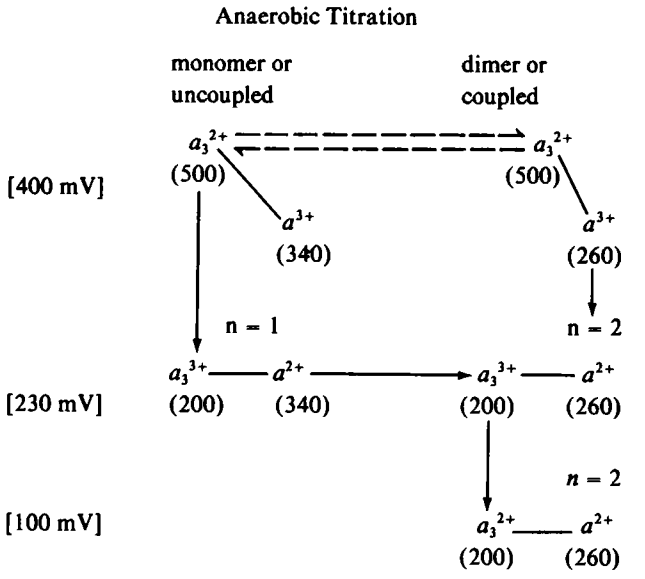

Scheme I

Two forms of the oxidase are envisioned, one uncoupled with heme *a* having an $E_m = 340$ mV and $n = 1$, the other with heme *a* in some coupled form with $E_m = 260$ mV and $n = 2$. The compatibility of our data with this model based on Nernstian components at equilibrium indicates that the reaction linking these two species does not alter the concentration of either species on the time scale of the experiment. In both states, when heme *a* is oxidized, heme a_3 has an E_m above that of $K_3F_e(CN)_6$, which is represented here arbitrarily as 500 mV. The numbers in parenthesis indicate E_m values. When heme *a* becomes reduced, the E_m of heme a_3 drops from 500 mV to ~200 mV. The mixed valence monomer is more stable in the dimeric or coupled form, and the reduction of heme a_3 then proceeds as an $n = 2$ step. Starting a reductive titration at 400 mV (E_h values shown on left in brackets) heme *a* is oxidized and heme a_3 reduced. This scheme explains the $n = 1$ titration seen at 340 mV and the observations that concomitant with the reduction of this center, a portion of the heme a_3 is oxidized because of the sudden drop of its E_m to 200 mV. (see troughs at 429 nm in Figs. 1 and 2). As the voltage is lowered, an $n = 2$ titration with an E_m of 260 mV is seen attended by the oxidation of more heme a_3 (see Figs. 1 and 2). Finally the newly oxidized heme a_3 is reduced as the titration continues, accounting for the growth of the Soret peak at 429 nm.

A possible drawback to the scheme we have proposed is the thermodynamic accounting for the relatively large changes envisioned for the E_m of heme a_3. However, the proposed mechanism is cyclic and we are still free to hypothesize that the negative free energy associated with the raising of the E_m of heme a_3 is stored at the same site from which it is expended later in the cycle to lower E_m by

the same amount. In the reaction catalyzed by the enzyme in which four electrons are transferred from reduced cytochrome *c* to oxygen, a total standard negative free energy change of 24 kcal occurs.

The new information presented in this work may help in the formulation of mechanisms to account for the catalytic ability of the enzyme. More importantly, the assignment of unique difference spectra to individual Nernstian centers should help in the interpretation of spectral changes seen during rapid kinetic measurements with the purified enzyme. In this connection, it is worth noting that the "fast phase" in the reduction of oxidized beef heart cytochrome oxidase by hexaammineruthenum II was accompanied by a spectral change quite similar to the difference spectra we have observed in our equilibrium titrations (Scott and Gray, 1980). In both cases prominent spectral changes at 429 and 448 nm were seen. Our technique for resolving total spectra should be useful in pursuing such a study.

The expert assistance of Olof Einarsdóttir in the isolation of the oxidase is gratefully acknowledged. The system for computer-controlled potentiostatic titrations was designed with the help of Walter S. Friauf. The authors have profited from many helpful discussions with David Bickar.

Isolation of the bovine cytochrome *c* oxidase was supported by USPHS Grant HL-15980 to W. S. Caughey.

Received for publication 21 March 1985 and in final form 29 August 1985.

REFERENCES

Caughey, W. S. 1967. Porphyrin proteins and enzymes. *Annu. Rev. Biochem.* 36:611–644.

Georgevich, S., V. M. Darley-Usman, F. Malatesta, and R. A. Capaldi. 1983. Electron transfer in monomeric forms of beef and shark heart cytochrome *c* oxidase. *Biochemistry.* 22:1317–1322.

Kumar, C., A. Naqui, and B. Chance. 1984. The identity of pulsed cytochrome oxidase. *J. Biol. Chem.* 259:2073–2076.

Leigh, J. S., D. F. Wilson, C. S. Owens, and T. E. King. 1974. Heme-heme interaction in cytochrome *c* oxidase: the cooperativity of the hemes of cytochrome *c* oxidase as evidenced in the reaction with CO. *Arch. Biochem. Biophys.* 160:476–486.

Lemberg, M. R. 1969. Cytochrome oxidase. *Physiol. Revs.* 49:48–121.

Malmström, B. G. 1974. Cytochrome *c* oxidase: some current biochemical and biophysical problems. *Quant. Rev. Biophys.* 6:389–431.

Nicholls, P., and L. C. Petersen. 1974. Haem-haem interactions in cytochrome aa_3 during the anaerobic-aerobic transition. *Biochim. Biophys. Acta.* 357:462–467.

Okunuki, K., B. Hagihara, I. Sekuzu, and T. Horio. 1957. Studies on cytochrome oxidase in *Proc. Intern. Symp. Enzyme Chemistry.* Tokyo and Kyoto, Maruzen, Tokyo. K. Schihara, editor. Academic Press Inc., NY. 1958. 264.

Reddy, K. V. Subba, and R. W. Hendler. 1983. Complete analysis of the cytochrome components in terms of spectra and redox properties: the *b*-type cytochromes. J. Biol. Chem. 258:8568–8581.

Reddy, K. V. Subba, and R. W. Hendler. 1986. Complete analysis of the cytochrome components of beef heart mitochondria in terms of spectra and redox properties: the c_1 cytochromes. *Biophys. J.* 49:693–703.

Reddy, K. V. Subba, R. W. Hendler, and B. Bunow. 1986. Complete analysis of the cytochrome components of beef heart mitochondria in terms of specra and redox properties: cytochromes aa_3. *Biophys. J.* 49:705–715.

Rieske, J. S., and S. H. K. Ho. 1985. Respiratory complex III: structural-functional relationships. *In* Coenzyme Q. G. Lenaz, editor. John Wiley & Sons, Ltd. Chichester, England. 337–363.

Scott, R. A., and H. B. Gray. 1980. Cytochrome aa_3 electron-transfer reactions. Kinetics of hexaammineruthenium (II) reduction of the beef-heart enzyme. *J. Am. Chem. Soc.* 102:3219–3224.

Shrager, R. I., and R. W. Hendler. 1982. Titration of individual components in a mixture with resolution of difference spectra, pKs, and redox transitions. *Anal. Chem.* 54:1147–1152.

Shrager, R. I., and R. W. Hendler. 1986. Processing and analysis of potentiometric data. *Biophys. J.* 49:687–691.

Wikström, M. K., H. J. Harmon, W. J. Ingledew, and B. Change. 1976. A re-evaluation of the spectral, potentiometric and, energy-linked properties of cytochrome *c* oxidase in mitochondria. *FEBS (Fed. Eur. Biochem. Soc.) Lett.* 65:259–277.

Wikström, M. K., K. Krab, and M. Saraste. 1981. Cytochrome Oxidase, A synthesis. Academic Press Inc., NY.

Wilson, E. F., and P. L. Dutton. 1970. Energy dependent changes in the oxidation-reduction potential of cytochrome *b**. *Biochem. Biophys. Res. Commun.* 39:59–64.

Wilson, D. F., J. G. Lindsay, and E. S. Bracklehurst. 1974. Heme-heme interaction in cytochrome oxidase. *Biochim. Biophys. Acta.* 256:277–286.

Yoshikawa, S., and W. S. Caughey. 1982. Heart cytochrome *c* oxidase: an infrared study of effects of oxidation state on carbon monoxide binding. *J. Biol. Chem.* 257:412–420.

Yoshikawa, S., M. G. Choc, M. C. O'Toole, and W. S. Caughey. 1977. An infrared study of CO binding to heart cytochrome *c* oxidase and hemoglobin A. *J. Biol. Chem.* 252:5498–5508.